

RESEARCH

Open Access



Asiatic acid attenuates methamphetamine-induced neuroinflammation and neurotoxicity through blocking of NF- κ B/STAT3/ERK and mitochondria-mediated apoptosis pathway

Ji-Hyun Park¹, Young Ho Seo¹, Jung-Hee Jang², Chul-Ho Jeong¹, Sooyeon Lee¹ and Byoungduck Park^{1*}

Abstract

Background: Methamphetamine (METH) is a commonly abused drug that may result in neurotoxic effects. Recent studies have suggested that involvement of neuroinflammatory processes in brain dysfunction is induced by misuse of this drug. However, the mechanism underlying METH-induced inflammation and neurotoxicity in neurons is still unclear. In this study, we investigated whether asiatic acid (AA) effected METH-mediated neuroinflammation and neurotoxicity in dopaminergic neuronal cells. And we further determined whether the effect involved in the nuclear factor kappa-light-chain-enhancer of activated B cells (NF- κ B) and signal transducer and activator of transcription (STAT) 3 and extracellular signal-regulated kinase (ERK) pathway.

Methods: We used the human dopaminergic neuroblastoma SH-SY5Y cell line, murine microglial BV2 cell line, and primary culture of rat embryo mesencephalic neurons. Pro-inflammatory cytokine production was monitored by ELISA and RT/real-time PCR. The cell cycle distribution and mitochondrial membrane integrity was analyzed by flow cytometry. We used immunoblotting, DNA-binding activity, and immunofluorescence staining to analyze the effect of AA on activation of the NF- κ B, STAT3, MAPK-ERK, and apoptosis signaling pathways.

Results: METH induced TNF receptor (TNFR) expression and led to morphological changes of cells. Additionally, this drug increased pro-inflammatory cytokine (TNF α and IL-6) expression. AA significantly suppressed METH-induced TNFR expression in concentration dependent. Increased secretion of TNF α and IL-6 was inhibited in METH-stimulated neuronal cells by AA administration. AA showed significant protection against METH-induced translocation of NF- κ B/STAT3 and ERK phosphorylation. AA inhibited METH-induced proteolytic fragmentation of caspase-3 and PARP. The pro-apoptotic protein Bax was significantly decreased, while the anti-apoptotic protein Bcl-xL was increased by AA treatment in METH-stimulated cells. A similar protective effect of AA on mitochondrial membrane integrity was also confirmed by flow cytometry and immunofluorescence staining.

Conclusions: Based on the literatures and our findings, AA is a promising candidate for an anti-neurotoxic agent, and it can potentially be used for the prevention and treatment of various neurological disorders.

Keywords: Methamphetamine, Asiatic acid, Neuroinflammation, Neurotoxicity, NF- κ B, STAT3, ERK

* Correspondence: bdpark@kmu.ac.kr

¹College of Pharmacy, Keimyung University, 1095 Dalgubeoldaero, Dalseo-Gu, Daegu 42601, Republic of Korea

Full list of author information is available at the end of the article



Background

Methamphetamine (METH) is a commonly abused drug that may result in neurotoxic effects, which contribute to neuronal damage and inflammation [1, 2]. It has been well-recognized that high doses of METH impair nigrostriatal dopaminergic systems in both rodents [3] and primates [4]. Although the pathogenesis of METH-induced dopaminergic neurotoxicity remains to be elucidated, this neurotoxicity may be, at least in part, related to oxidative stress [5, 6], inflammatory changes [7], and apoptosis [8]. METH may act upon neurons as a central processor of inflammation by releasing pro-inflammatory molecules [9]. These pro-inflammatory molecules may further activate downstream apoptotic signaling pathways in neurons, ultimately resulting in neuronal death and/or the activation of glial cells, which can further exacerbate neuroinflammation. In addition, the pathogenesis of dopaminergic neurotoxicity observed in Parkinson's disease (PD) is similar to the neuroinflammatory and neurotoxic effect of METH [10].

Several studies have reported the neurotoxic mechanism of METH, including oxidative stress and apoptosis in neuronal cells [11–13]. METH causes induction of pro-inflammatory mediators such as inducible nitric oxide synthase (iNOS), interleukin (IL)-1 β , IL-6, and tumor necrosis factor (TNF)- α [1, 14, 15]. Specifically, TNF α has been reported to be a potent stimulator of IL-6 production, whose pleiotropic action can be through the TNF receptor (TNFR) [9]. The activation of TNFR stimulates several signaling pathways that regulate cellular processes, ranging from cell proliferation and differentiation to cell death [16]. With respect to IL-6, its production seems to be regulated by several signaling cascades [9, 17], including TNF- α activation via the nuclear factor kappa-light-chain-enhancer of activated B cells (NF- κ B) and signal transducer and activator of transcription (STAT) signaling pathways [14, 15, 18].

Increasing evidence has revealed that METH-induced neurodegeneration is associated with mitochondria-dependent apoptosis [19]. In addition, administration of METH in mice has been shown to cause an increase in pro-apoptotic proteins (BAX, BAD, and BID) but a decrease in anti-apoptotic Bcl-2-related proteins [11]. METH-induced alterations in these proteins have been suggested to form channels that result in mitochondrial membrane potential loss and allow cytochrome c release [20]. These observations propose that mitochondrial damage may contribute to METH-induced neurotoxicity. A direct cytotoxic role of METH has been found to be mediated by the mitogen-activated protein kinase (MAPK) pathway followed by the activation of caspases and the induction of apoptosis [21]. Although extensive research has focused on development of pharmacological agents that inhibit METH-induced neurotoxicity,

FDA-approved pharmacotherapies for the treatment of negative effects of METH are still lacking [22]. Novel approaches aimed at overcoming the negative effects of METH are urgently needed in this field.

Asiatic acid (AA), a natural pentacyclic triterpene derived from the medicinal herb *Centella asiatica*, elicits multiple bioactivities, including antioxidant, anti-apoptotic, and anti-inflammatory properties [23–26]. A previous study showed that AA attenuates glutamate-induced cognitive deficits in mice and apoptosis in human neuroblastoma dopaminergic SH-SY5Y cells [27]. AA improves learning and memory in an animal model, which was correlated with an increase in hippocampal neurogenesis [28–30]. Although studies on the physiological function of AA, including anti-inflammatory and anti-apoptotic functions, were performed, the effectiveness of AA related to METH-induced neurotoxicity has not been evaluated. Therefore, in this study, we investigated the potential therapeutic effects of AA on the production of pro-inflammatory cytokines induced by METH. We also evaluated the molecular impact of AA on the signal transduction pathways involved in METH-induced neurotoxicity.

Methods

Cell cultures and reagents

A dopaminergic human neuroblastoma cell line SH-SY5Y (America Tissue Culture Collection, CRL-2266; ATCC, VA, USA) was cultured in a Dulbecco's modified Eagle's medium (DMEM) (Gibco, NY, USA) containing 10% fetal bovine serum (FBS; Gibco) and 1% Anti-Anti (Gibco). BV-2 murine microglia cells, a generous gift from Dr. Hoe (Korea Brain Research Institute, KBRI), were cultured in DMEM containing 10% FBS and 0.1% gentamicin (Gibco). Mesencephalic neuron cultures were prepared from the ventral mesencephalic tissues of embryonic day 13–14 rats, as described previously [31]. All experimental protocols were approved by the Institutional Animal Care and Use Committee of the Keimyung University (Daegu, South Korea; EXP-IRB number: KM_2016-007; the date of approval: 1 April 2016) in accordance with the criteria outlined in the Institutional Guidelines for Animal Research. Briefly, dissociated cells were seeded at 1×10^5 /well to poly-D-lysine- and laminin-coated 24-well plates. Cells were cultured in a Dulbecco's modified Eagle's medium/Ham's F-12 medium (Gibco) containing ITS premix (Sigma-Aldrich, MO, USA) and 1% penicillin-streptomycin (Gibco). Cell cultures were maintained at 37 °C in a humidified atmosphere of 5% CO₂.

Methamphetamine (METH) was purchased from the Ministry of Food and Drug Safety (Korea). Asiatic acid (AA) was purified and received from Dr. Ki Yong Lee, a professor of the College of Pharmacy, Korea University. Signal inhibitors were obtained from Sigma-Aldrich (MO, USA).

Morphological examination

Morphological changes in cells were observed under an inverted phase-contrast microscope (Leica, Germany). The effect of AA on METH-induced neuroinflammation was observed for 24 h, and METH-induced neurotoxicity was observed for 12 h. The photographs were taken at $\times 200$ or $\times 400$ magnification using a digital camera.

Cytotoxicity assay

Cells were plated in 96-well culture plates at 1×10^6 cells/ml in culture medium and allowed to attach for 24 h. Media were then discarded and replaced with new medium containing various concentrations of METH and AA. The cells were cultured for an additional 24 h, and then, 3-(4,5-dimethylthiazol-2-yl)-2,5-diphenylterazolium bromide (MTT, 5 mg/ml; Sigma-Aldrich) was added to each well (1/10 of medium volume), and the samples were incubated at 37 °C in a 5% CO₂ incubator for 4 h. The formazan precipitate was dissolved in dimethyl sulfoxide (DMSO), and absorbance was measured at 540 nm using a microplate reader (Bio-Rad Laboratories, CA, USA).

Treatment kinase inhibitors and siRNA transfection

Cells were pretreated with various inhibitors (Sigma-Aldrich) such as NF- κ B-specific inhibitor: Bay11-7085 (20 μ M), STAT3-specific inhibitor: S3I-201 (20 μ M), and ERK1/2-specific inhibitor: PD98059 (20 μ M). After 1 h, the cells were treated and co-cultured with METH for 24 h. Cells were transfected with control siRNA (Cat no: sc-37007, Santa Cruz, CA, USA) and ERK-MAPK siRNA (Cat no: 6560, Cell Signaling Technology, MA, USA) using Lipofectamine RNAiMAX transfection reagent (Invitrogen) according to the manufacturer's instruction.

Enzyme-linked immunosorbent assay (ELISA)

The culture medium of the cells was harvested, and cytokine production (TNF α and IL-6) in the supernatant was measured with a solid-phase sandwich enzyme-linked immunosorbent assay (ELISA) using a Quantikine TNF- α and IL-6 kit (R&D systems, MN, USA) according to the manufacturer's instructions.

Immunoblot analysis

Cytosolic and nuclei protein fractions were obtained as described [32]. The protein concentration was determined with a Bio-Rad Bradford kit (Bio-Rad Laboratories, CA, USA). The samples were boiled for 5 min, and equal volumes were loaded on a sodium dodecyl sulfate-polyacrylamide gel electrophoresis (SDS-PAGE). The resolved proteins were transferred onto a nitrocellulose membrane and probed with anti-TNFR, anti-p-NF- κ B p65, anti-NF- κ B p65, anti-p-STAT3, anti-STAT3, anti-p-JAK2, anti-JAK2, anti-p-ERK1/2, anti-ERK1/2, anti-p-JNK1/2, anti-JNK1/2, anti-p-p38, anti-p38, anti-TH,

anti-lamin B, and anti- β -actin (all from Cell Signaling Technology) followed by a secondary antibody conjugated to horseradish peroxidase and detected with enhanced chemiluminescence reagents (Amersham Bioscience, UK). The luminescent signals were analyzed using an ImageQuant LAS 4000 Scanner of GE Healthcare (Piscataway, NJ, USA).

Reverse-transcription and real-time PCR

Total RNA was extracted from neuronal cells with TRIzol reagent (Invitrogen Co, Grand Island, NT, USA) according to the manufacturer's instructions. First-strand cDNA was synthesized with oligo-d(T) primer and M-MLV reverse transcriptase (Promega, Madison, WI, USA). Real-time PCR was performed in a CFX 96 Touch™ detection system (Bio-Rad Laboratories) using SYBR Green PCR Master Mix (Bio-Rad Laboratories). Each measurement was repeated at least in triplicate, and the relative quantity of target mRNA was determined using the comparative threshold (C_t) method by normalizing target mRNA C_t values to those for β -actin (ΔC_t). Aliquots of cDNA were used for PCR using primer sets specific to TNF- α , IL-6, and β -actin as a control. Used primers are as follows: for TNF- α , 5'-TCT CGA ACC CCG AGT GAC AA-3' (sense) and 5'-TGA AGA GGA CCT GGG AGT AG-3' (antisense); for IL-6, 5'-CAC AGA CAG CCA CTC ACC TC-3' (sense) and 5'-TTT TCT GCC AGT GCC TCT TT-3' (antisense); and for β -actin, 5'-CTT CCT GGG CAT GGA GTC CT-3' (sense) and 5'-GGA GCA ATG ATC TTG ATC TT-3' (antisense).

Electrophoretic mobility shift analysis (EMSA) and supershift assay

As described in our previous studies, the DIG Gel Shift Kit (Roche, Mannheim, Germany) was used to detect NF- κ B-p65- and STAT3-binding activity, with the instructions of the manufacturer [32, 33]. The binding activity of NF- κ B-p65 and STAT3 in the METH-induced cells was confirmed by EMSA or supershift assay with a DIG-labeled oligonucleotide (NF- κ B: 5'-AGT TGA GGG GAC TTT CCC AGG C-3', STAT3: 5'-CTT CAT TTC CCG TAA ATC CCT AAA GCT-3') and NF- κ B-p65 and STAT3 antibody (Cell Signaling Technology). The NF- κ B-p65-oligo, NF- κ B-p65-Ab, STAT3-oligo, and STAT3-Ab complexes were separated by electrophoresis on 6% non-denaturing polyacrylamide gels. After electrophoresis, the gels were transferred to nylon membranes and detected by chemiluminescence. The luminescent signals were analyzed on an ImageQuant LAS 4000 Scanner (GE Healthcare).

Immunofluorescence staining

Cells were grown on chamber slides and coating cover slides and fixed with 3.7% paraformaldehyde in PBS. The

membrane was permeabilized by treating cells for 2 min with 0.1% Triton X-100 in PBS. The cells were then placed in blocking solution (5% FBS in PBS) at room temperature. Cells were incubated with primary antibodies for 1 h at room temperature. After washing, they were incubated with the Alexa Flour 488 (excitation/emission = 495/519 nm, green, Invitrogen, CA, USA) and Alexa Flour 594 (excitation/emission = 590/617 nm, red, Invitrogen, CA, USA) for 30 min at room temperature. Cells were counterstained with Hoechst 33342 (excitation/emission = 330–380 nm/460 nm, ImmunoChemistry, MN, USA). Slides were mounted using ProLong[®] Gold antifade reagent (Molecular Probes[®] by Life Technologies[™], CA, USA). Primary antibodies utilized are the following: anti-pNF- κ B, anti-pSTAT3, and anti-tyrosine hydroxylase (TH) (from Cell Signaling Technology). Immunolabeling was examined using an Eclipse Ti-U and confocal microscope (Nikon, Tokyo, Japan).

Annexin V/propidium iodide (PI) staining

Apoptotic cells were differentiated from viable or necrotic cells using a combined staining of annexin V-FITC and PI (Invitrogen). To investigate the neurotoxic effect of AA on METH, cells were pretreated with 20 μ M AA for 1 h and then exposed to 1.5 mM METH for 12 h. After the cells were trypsinized, they were washed in PBS and resuspended in annexin-binding buffer. The cell suspension (1×10^5 cells/ml) was incubated with FITC-conjugated anti-annexin V and PI for 15 min in the dark. Cells were counted using a BD FACSVerse[™] (BD Biosciences, NJ, USA) and analyzed by Flowing 2.5 version software. A total number of 10,000 events were recorded for each sample. The fluorescence spectrum of annexin V and PI were detected using a 527/32-nm and a 586/42-nm filter, respectively.

JC-1 mitochondrial transmembrane potential assay

To measure the mitochondrial transmembrane potential, JC-1 dye (Sigma-Aldrich), a sensitive fluorescent probe, was used. Fluorescence microscopy with a 488-nm filter was used for the excitation of JC-1. Emission filters of 535 and 595 nm were used to quantify the population of mitochondria with green (JC-1 monomers) and red (JC-1 aggregates) fluorescence, respectively. Immunolabeling was examined by an Eclipse Ti-U microscope (Nikon) and BD FACS Verse flow cytometer.

Statistical analysis

All values are expressed as mean \pm standard error of the mean (SEM). All data analysis was performed with the GraphPad Prism 5 (GraphPad Software, Inc., San Diego, CA) using either a one-way ANOVA with Tukey's post hoc test for multiple comparisons, with $p < 0.05$ defined as significant. For the quantification of immunofluorescence,

staining results are expressed as percentages of total cells stained with Hoechst 33342 per each field (n = number of fields). For all data, n corresponds to the number of independent experiments.

Results

Effects of AA on METH-induced production of pro-inflammatory cytokines

To determine cytotoxicity, dopaminergic SH-SY5Y cells (human neuroblastoma) treated with different concentrations of METH (0.5 to 5 mM) and AA (1 to 30 μ M) for 24 h were analyzed by an established MTT assay. The treatment of SH-SY5Y cells with AA concentrations ranging from 1 to 20 μ M showed mild growth inhibitory activity with a 10% decrease in cell viability at 20 μ M but exhibited some toxicity at 30 μ M (45%; Additional file 1: Figure S1a). The next experiment was performed to observe the viability and TNF α secretion of SH-SY5Y cells treated with METH for 24 h. Viability of METH-stimulated SH-SY5Y cells was decreased by about 30% as compared to that of control cells at 1 mM (Additional file 1: Figure S1b—upper). TNF α secretion was increased at 1 mM METH, and this was maintained similarly from 1.5 to 5 mM (Additional file 1: Figure S1b—lower). AA significantly increased the viability of 1 mM METH-stimulated SH-SY5Y cells in a concentration-dependent manner compared to that of cells treated with 1 mM METH alone (Additional file 1: Figure S1c). We also confirmed these results at the cell morphology level (Additional file 1: Figure S1d). SH-SY5Y cells showed healthy morphology with full cell bodies and extending neurites. After exposed to 1 mM METH, cells were sparsely distributed and displayed growth inhibition and development of short neurites with few branches. However, 20 μ M AA significantly inhibited the cell damage of 1 mM METH-stimulated SH-SY5Y cells. This result is consistent with changes of cell viability. Based on these results, the optimal AA concentration for subsequent experiments was chosen as 20 μ M for 1 mM METH-stimulated SH-SY5Y cells.

METH leads to rapid upregulation of pro-inflammatory cytokines such as TNF α and IL-6 through TNFR [9]. To determine whether AA can regulate METH-induced TNFR expression, SH-SY5Y cells were incubated in the presence or absence of AA for 1 h and then treated with METH for 24 h. AA significantly suppressed METH-induced TNFR expression in a concentration dependent (Fig. 1a). We next analyzed the effect of AA on METH-induced secretion of TNF α and IL-6 by ELISA. Increased TNF α and IL-6 secretion was significantly inhibited in METH-stimulated SH-SY5Y cells by AA administration (Fig. 1b). We also confirmed these results at the mRNA level. Consistent with the ELISA results, AA strongly suppressed METH-induced TNF α and IL-6 mRNA expression (Fig. 1c, d). Taken

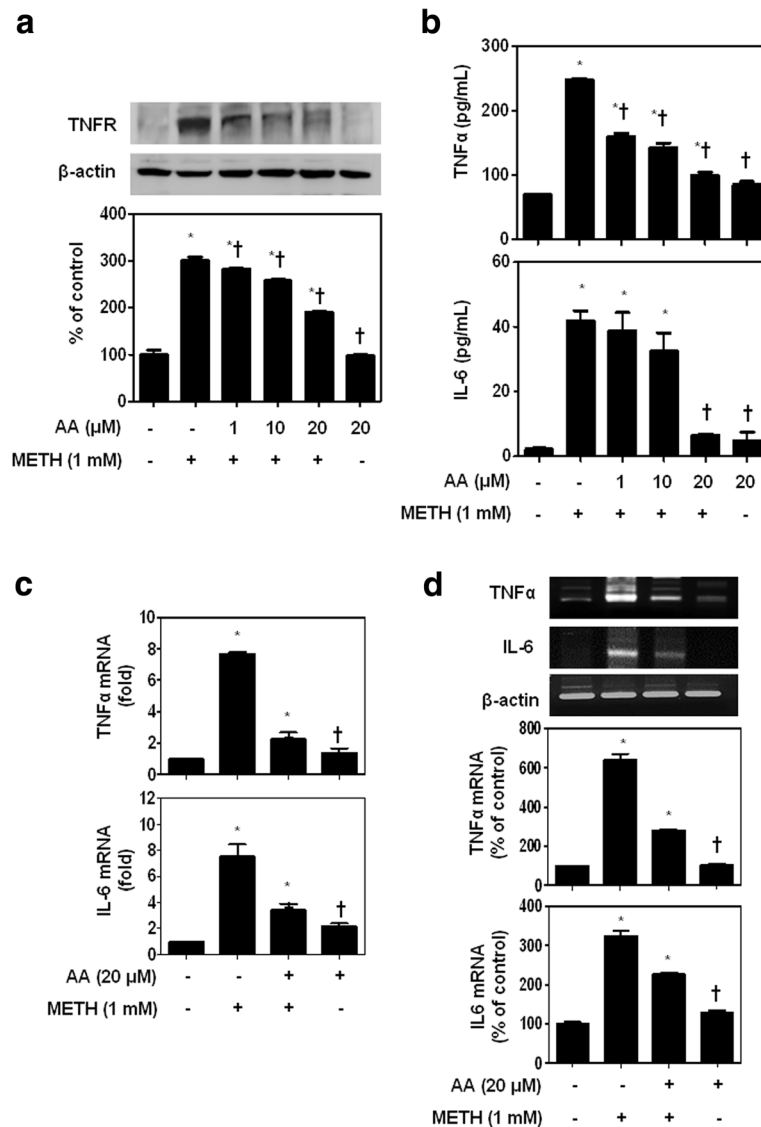


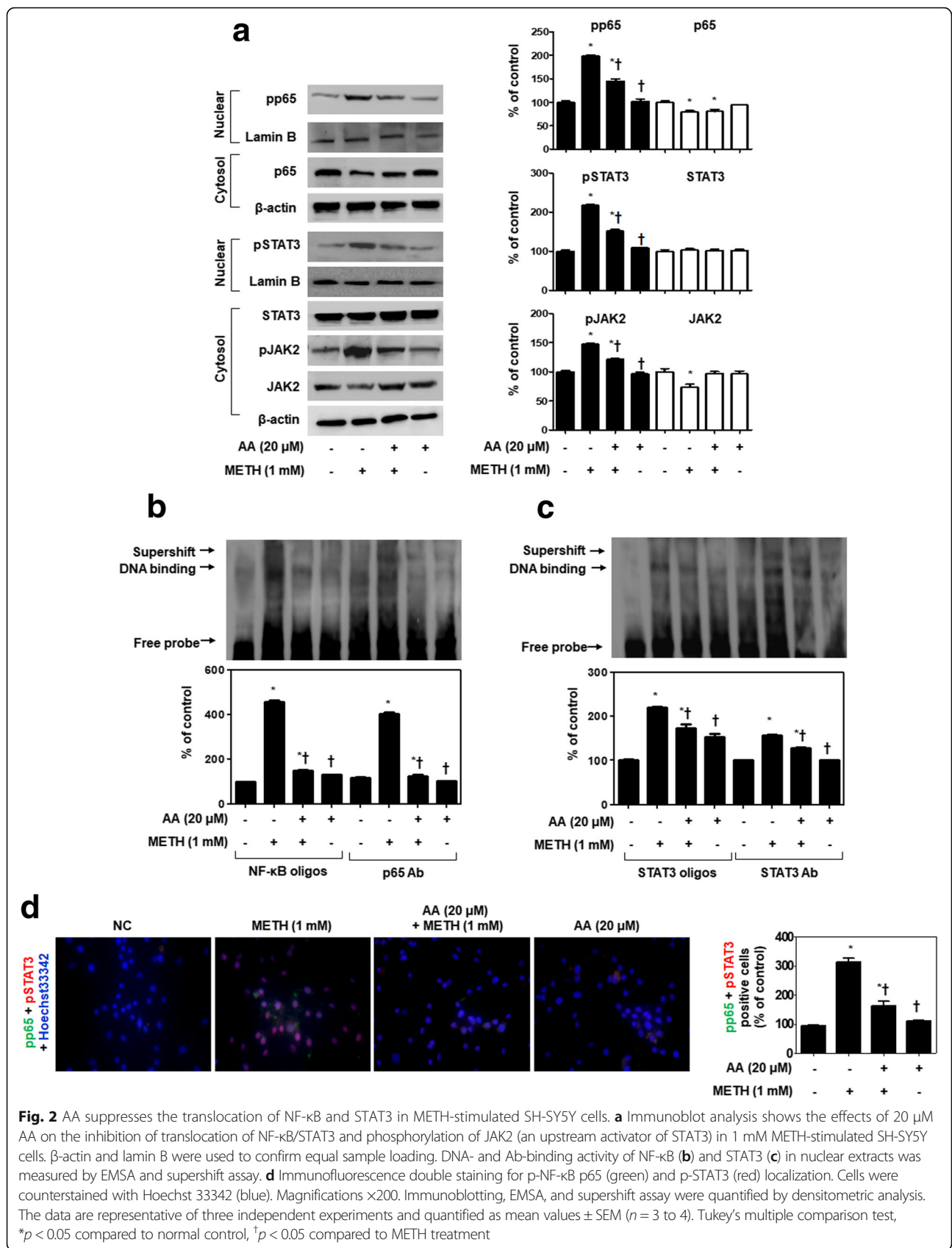
Fig. 1 AA inhibits METH-induced TNF-alpha and IL-6 production and mRNA expression levels. SH-SY5Y cells were incubated in the presence or absence of AA (1, 10, and 20 μM) for 1 h and then treated with 1 mM METH for 24 h. **a** TNFR overexpression was significantly inhibited in METH-stimulated SH-SY5Y cells by AA administration. AA strongly suppressed METH-induced TNFα and IL-6 production both in extracellular (**b**) and mRNA levels (**c, d**). β-actin was used to confirm equal sample loading. The data are representative of three independent experiments and quantified as mean values ± SEM (*n* = 4 to 9). Tukey's multiple comparison test, **p* < 0.05 compared to normal control, †*p* < 0.05 compared to METH treatment

together, our results indicate that AA inhibits METH-induced expression of TNFα and IL-6 at the level of mRNA, which resulted in inhibition of the pro-inflammatory cytokine production in dopaminergic SH-SY5Y cells.

AA inhibits pro-inflammatory cytokine secretion through suppression of NF-κB, STAT3, and ERK pathway

NF-κB and STAT3 activation is known to be a regulatory mechanism for TNFα and IL-6 [34]. Therefore, we examined the translocation of NF-κB and STAT3 in response to METH-induced neuroinflammation to

SH-SY5Y cells (Fig. 2a). SH-SY5Y cells were pretreated with 20 μM AA for 1 h and then stimulated with 1 mM METH for 24 h. Along with phosphorylation, NF-κB-p65 and STAT3 were translocated from the cytoplasm to the nucleus after METH stimulation, but this was effectively inhibited by AA. Moreover, AA strongly reduced METH-induced phosphorylation of JAK2. We further evaluated the effects of AA on METH-induced NF-κB and STAT3 DNA-binding activity (Fig. 2b, c). The nuclear extracts of SH-SY5Y cells, which were incubated in the presence or absence of AA, were analyzed using DIG-labeled oligonucleotides corresponding to the NF-κB and STAT3 sites.



Formation of NF- κ B-DNA, NF- κ B-Ab, STAT3-DNA, and STAT3-Ab complexes was prominent in nuclear extracts from METH-stimulated SH-SY5Y cells. However, formation of these complexes was significantly suppressed in METH-stimulated SH-SY5Y cells when these cells were treated with AA. We performed immunofluorescence staining to confirm whether treatment with AA could inhibit nuclear translocation of NF- κ B and STAT3 (Fig. 2d, Additional file 2: Figure S2). The translocation of NF- κ B and STAT3 was observed at the same position as the staining nucleus in METH-stimulated SH-SY5Y cells. These expressions were effectively inhibited by 20 μ M AA. The results were entirely consistent with our earlier data.

The MAPK signaling pathway, ERK-JNK-p38 MAPKs, is involved in the regulation of pro-inflammatory cytokines [35]. Previous reports have revealed that METH administration can increase the expression of ERK and JNK in the brain [7, 21]. Accordingly, we investigated whether 20 μ M influences 1 mM METH-induced pro-inflammatory cytokine expression via regulation of the ERK-JNK-p38 signaling pathway (Fig. 3a). Phosphorylation of ERK-JNK-p38 was significantly induced in METH-stimulated SH-SY5Y cells. AA inhibited METH-induced phosphorylation of ERK and JNK. However, phosphorylation of p38 was not affected. Interestingly, AA strongly inhibited METH-induced phosphorylation of ERK.

To confirm our finding that AA inhibits METH-induced pro-inflammatory cytokine expression through NF- κ B, STAT3, and MAPK-ERK signaling, we performed the following experiment after treatment of cells with inhibitors of NF- κ B (Bay11-7085), STAT3 (S3I-201), and ERK (PD98059). Consistent with the findings described above, Bay11-7085, S3I-201, PD98059, and AA significantly decreased METH-induced TNF α and IL-6 secretion and reduced these cytokines at the mRNA level (Fig. 3b, c).

To further investigate the role of ERK in METH-induced translocation of p65 and STAT3, cells were transfected with ERK siRNA or treated with the ERK inhibitor (PD98059). As shown in Fig. 3d, METH-induced translocation of p65 and STAT3 was inhibited when the ERK pathway of these cells was downregulated. Together, these data suggest that AA inhibits translocation of NF- κ B/STAT3 and suppresses ERK phosphorylation, ultimately leading to inhibition of METH-induced pro-inflammatory cytokine production.

AA inhibits the NF- κ B, STAT3, and MAPK-ERK signaling pathway in METH-stimulated BV2 cells

Microglia activation and the release of various inflammatory cytokines are largely related to neurological diseases [36]. Accordingly, we explored whether AA influences pro-inflammatory cytokine production via

regulation of NF- κ B, STAT3, and MAPK-ERK signaling pathways in microglia BV2 cells. BV2 cells were pretreated with 20 μ M AA for 1 h and then stimulated with 1 mM METH for 24 h. In agreement with the results in Figs. 2 and 3, 1 mM METH strongly induced translocation of p65 and pSTAT3 in BV2 cells (Fig. 4a). In addition, phosphorylation of JAK2, an upstream activator of STAT3, and ERK was induced by METH in BV2 cells. Twenty micromolar of AA inhibited 1 mM METH-induced translocation of NF- κ B/STAT3 and phosphorylation of JAK2/ERK in BV2 cells.

It was further investigated whether AA affects METH-induced pro-inflammatory cytokine secretion through NF- κ B, STAT3, and MAPK-ERK signaling. BV2 cells were pretreated with 20 μ M AA or inhibitors (20 μ M Bay11-7085, 20 μ M S3I-201, 20 μ M PD98059) for 1 h and then stimulated with 1 mM METH for 24 h. When we examined the effects of AA on METH-induced pro-inflammatory cytokine expression following treatment with Bay11-7085, S3I-201, PD98059, and AA, these all significantly decreased METH-induced TNF α and IL-6 secretion (Fig. 4b). Subsequently, we examined whether 20 μ M AA inhibits 1 mM METH-induced NF- κ B and STAT3 DNA-binding activity (Fig. 4c, d). Increased formation of NF- κ B-DNA and STAT3-DNA complexes was suppressed in 1 mM METH-stimulated BV2 cells with 20 μ M AA treatment. Together, these results indicate that AA strongly inhibits METH-induced pro-inflammatory cytokine expression in microglia cells.

AA inhibits the neuroinflammatory pathway in METH-stimulated tyrosine hydroxylase (TH)-positive neurons

Primary neuronal cells were obtained from the ventral mesencephalic tissues of embryonic day 13–14 rats. Cultures of mesencephalic neurons are widely used as a source of dopaminergic neurons for the study of mechanisms implicated in dopaminergic cell death and for the evaluation of potential dopaminergic neuroprotective agents, including neurotrophic factors [37]. Therefore, we next analyzed the effect of AA on METH-induced secretion of pro-inflammatory cytokines and the translocation of NF- κ B and STAT3 in mesencephalic neurons. These neurons were pretreated with AA for 1 h and then stimulated with METH for 24 h. In the presence or absence of AA, the morphological changes in dopaminergic neurons after exposure to METH were observed under an inverted microscope (Fig. 5a—upper). The normal control cells grew well showing obvious neurites, and the cells treated with AA alone did not show any difference in cell growth when compared with normal cells. When TH-positive neurons were exposed to METH, neurites were reduced and cell debris was increased; however, they were recovered with AA co-treatment.

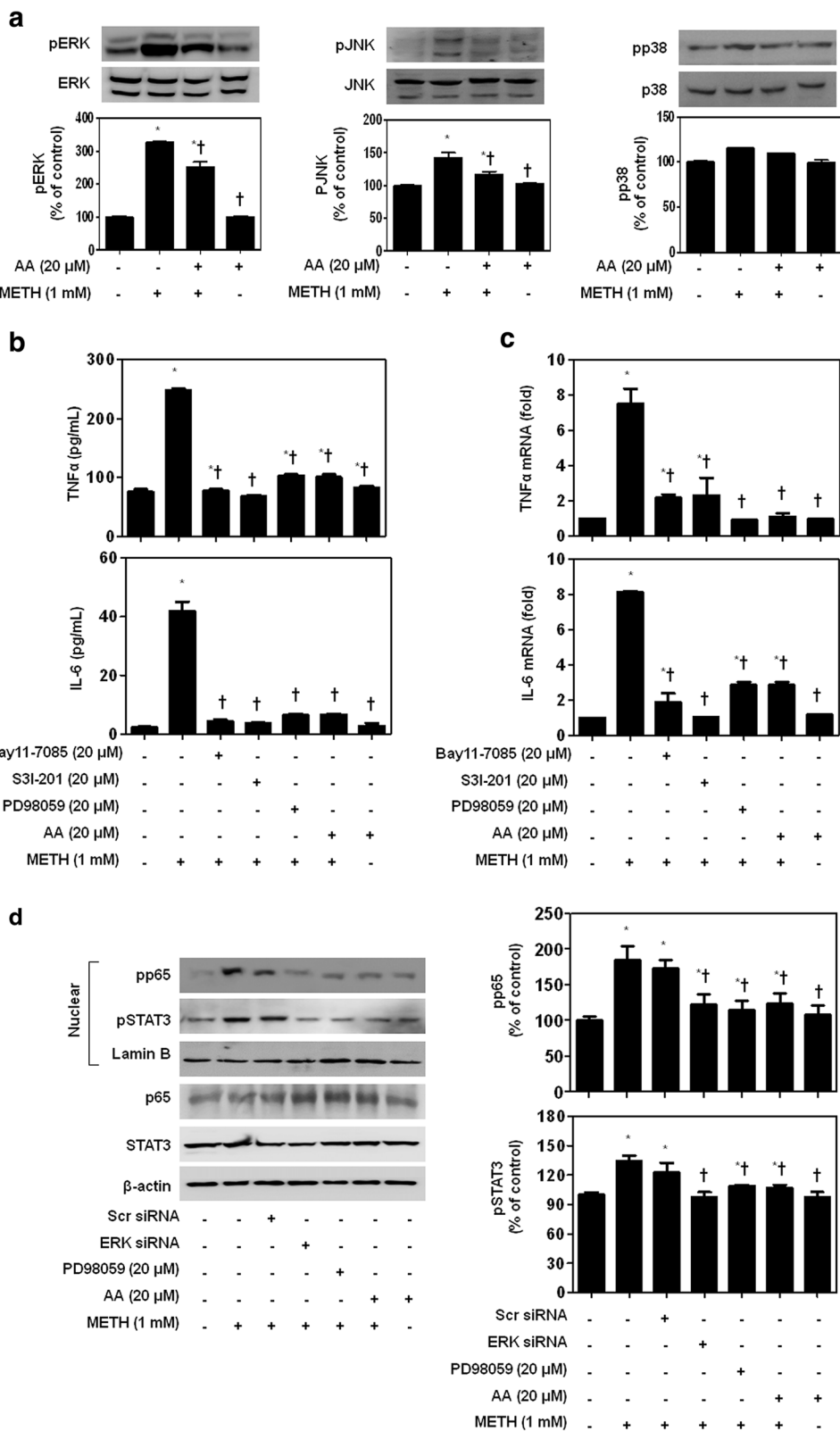


Fig. 3 (See legend on next page.)

(See figure on previous page.)

Fig. 3 AA inhibits pro-inflammatory cytokine secretion through suppression of NF- κ B, STAT3, and ERK pathway in METH-stimulated SH-SY5Y cells. SH-SY5Y cells were pretreated with 20 μ M AA or various inhibitors for 1 h and then stimulated with 1 mM METH for 24 h. **a** Phosphorylation of ERK was strongly inhibited in METH-stimulated SH-SY5Y cells by AA administration. Inhibitors of NF- κ B (Bay11-7085), STAT3 (S3I-201), ERK (PD98059), or AA strongly suppressed METH-induced TNF α and IL-6 production both in extracellular (**b**) and mRNA levels (**c, d**). METH-induced translocation of p65 and STAT3 was inhibited when the ERK pathway of these cells were downregulated. β -actin and lamin B were used to confirm equal sample loading. Immunoblotting was quantified by densitometric analysis. The data are representative of three independent experiments and quantified as mean values \pm SEM ($n = 4$ to 6). Tukey's multiple comparison test, * $p < 0.05$ compared to normal control, † $p < 0.05$ compared to METH treatment

These results show that AA exerts a protective effect against cell damage induced by METH. Immunofluorescence analysis with an antibody against TH revealed that mesencephalic neuronal cells were healthy TH-positive neurons with extensive neurites (Fig. 5a—lower). However, treatment of neurons with METH for 24 h reduced the number of TH-positive cells. When the cells were treated with AA alone, the number and morphology of the TH-positive neurons were not changed. The addition of AA to METH-treated cells seemed to protect against the loss of TH-positive neurons. We also confirmed this result at the protein level. Consistent with immunofluorescence staining, 1 mM METH strongly induced TH reduction in mesencephalic neurons. This reduction was strongly reversed by AA in METH-stimulated mesencephalic neurons (Fig. 5b). In addition, AA showed significant inhibition against METH-induced phosphorylation of ERK and translocation of NF- κ B/STAT3 in mesencephalic neurons.

Next, we further investigated whether Bay11-7085, S3I-201, and AA play a role in regulating METH-induced pro-inflammatory cytokine production. Mesencephalic neurons were pretreated with 20 μ M AA or inhibitors (20 μ M Bay11-7085, 20 μ M S3I-201, 20 μ M PD98059) for 1 h and then stimulated with 1 mM METH for 24 h. As shown in Fig. 5c, secretion of TNF α by METH was slightly higher in mesencephalic neurons than the SH-SY5Y and BV2 cells. Bay11-7085, S3I-201, PD98059, and AA significantly decreased secretion in METH-stimulated mesencephalic neurons. Accordingly, METH-induced IL-6 secretion was also decreased by AA or inhibitors. To confirm our results, we conducted immunofluorescence staining using pNF- κ B and pSTAT3 antibodies (Fig. 5d, Additional file 3: Figure S3 and Additional file 4: Figure S4). Consistent with the findings presented above, localization of pNF- κ B and pSTAT3 to the nucleus was suppressed in METH-stimulated mesencephalic neurons by AA.

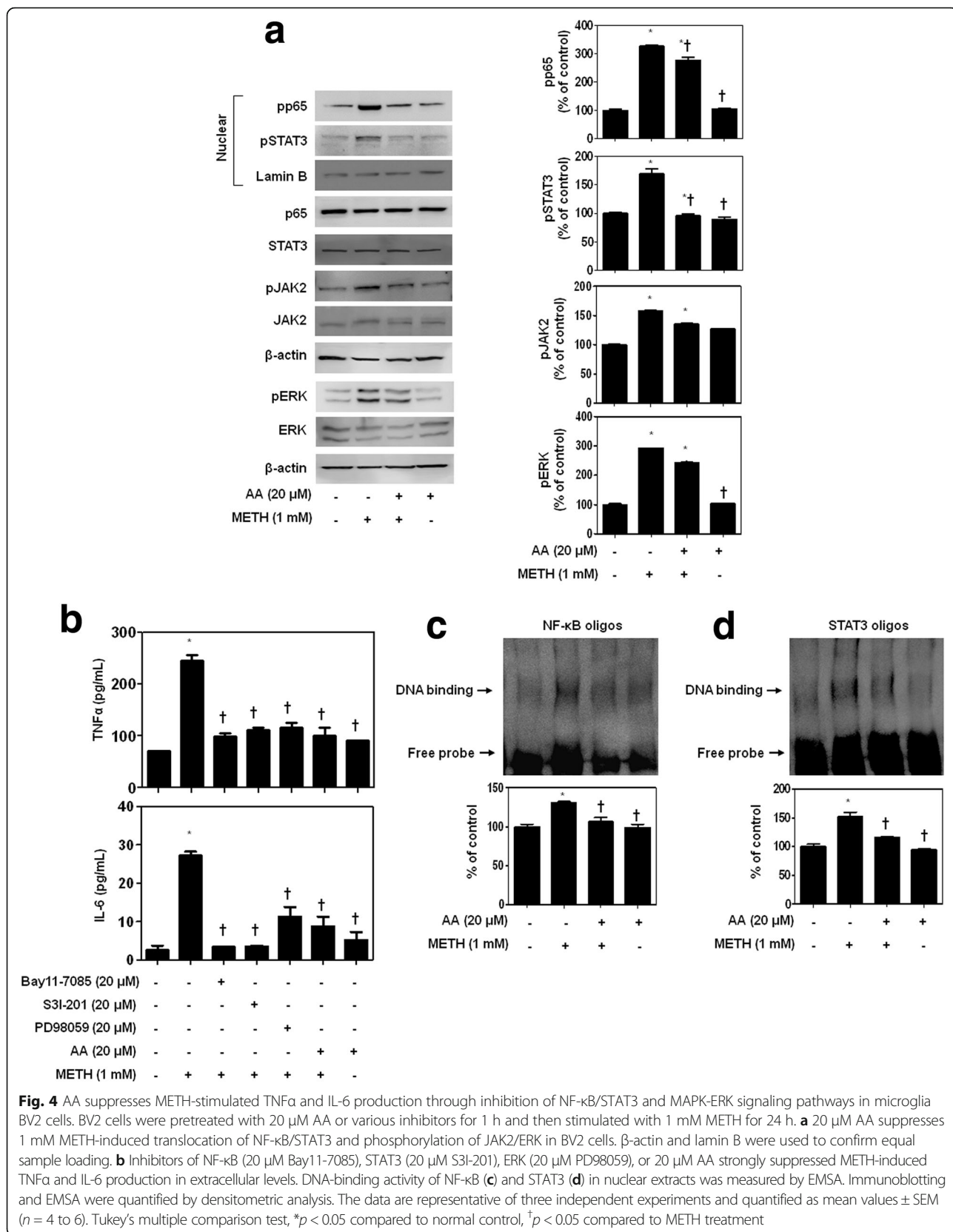
AA ameliorates METH-induced neurotoxicity in dopaminergic SH-SY5Y cells

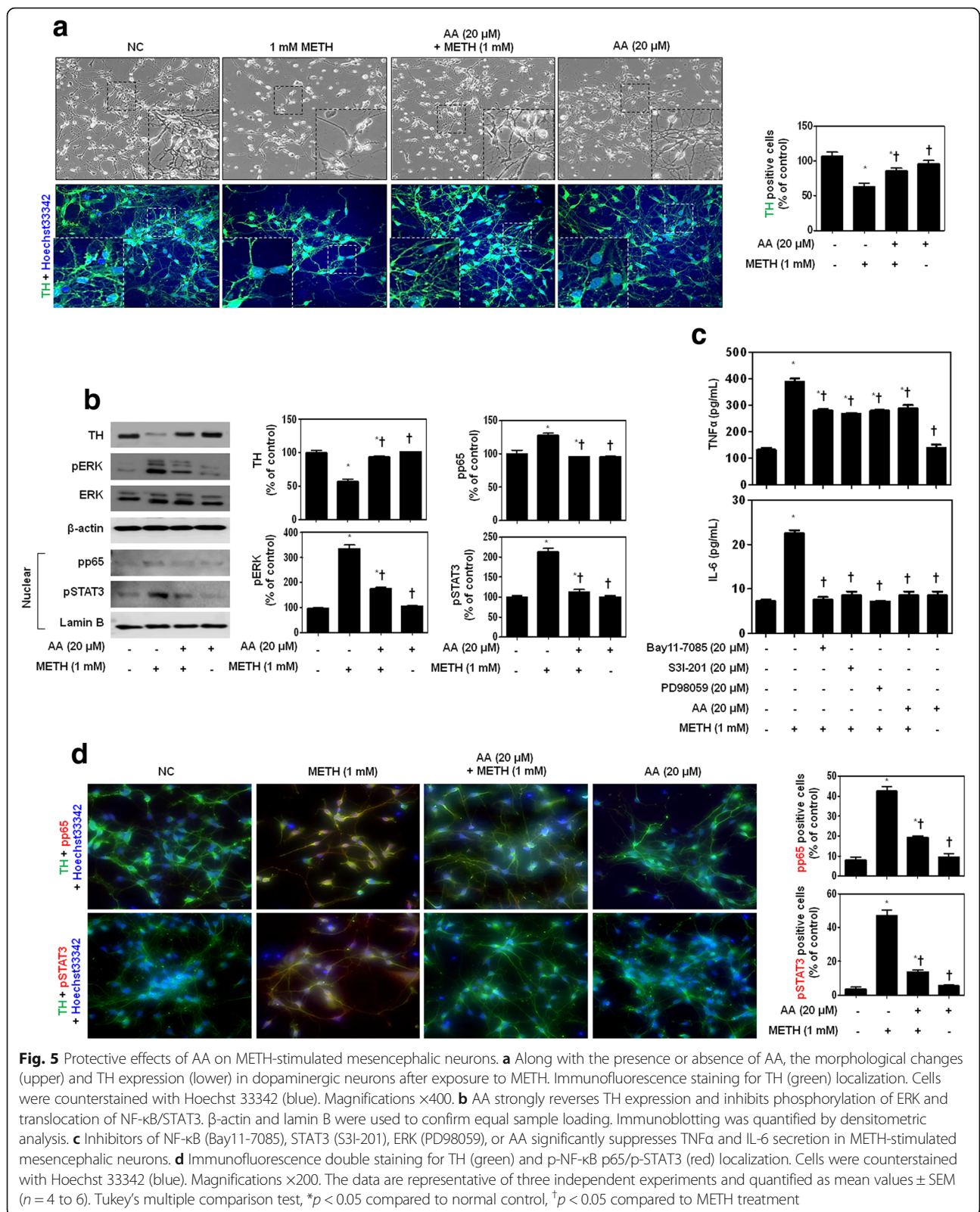
METH-induced apoptosis in neuronal cells is associated with the activation of NF- κ B, STAT3, and MAPK-ERK signaling [15, 18, 38]. We first analyzed the caspase-3 (17 kDa) and PARP (89 kDa) expression to understand the neurotoxic effects of METH on the growth of

dopaminergic SH-SY5Y cells (Additional file 5: Figure S5). We treated SH-SY5Y cells with METH (0.5, 1, 1.5, 2, and 5 mM) for 12 h and then conducted immunoblotting and examined cell morphology. METH-stimulated SH-SY5Y cells showed increased cleavage of caspase-3 (17 kDa) and PARP (89 kDa) in a concentration dependent. Full length of PARP was slightly detected from 2 mM of METH treated cells. So 1.5 mM of METH was chosen to confirm the inhibitory effect on METH neurotoxicity.

Next, to determine the effect of AA, the distribution of apoptosis cells by METH conducted flow cytometry with annexin V/PI staining. Flow cytometric analyses showed that 35.8% of the METH-stimulated SH-SY5Y cells stained positively for annexin V. However, only 1.54% cells treated with AA prior to METH stained positively for annexin V. These results suggested that AA increases cell viability and inhibits apoptosis of METH-stimulated SH-SY5Y cells (Fig. 6a). METH-stimulated SH-SY5Y cells showed increased cleavage of caspase-3 (17 kDa) and PARP (89 kDa). The addition of AA inhibited METH-induced proteolytic fragmentation of caspase-3 and PARP (Fig. 6b).

To evaluate the effects of METH on the production of apoptotic proteins related to mitochondria, we assessed Bcl-2 family activation in METH-treated SH-SY5Y cells by immunoblot analysis. As shown in Fig. 6c, the pro-apoptotic protein Bax was significantly decreased, while the anti-apoptotic protein Bcl-xL was increased by AA treatment. Next, we used JC-1 staining to measure the mitochondrial membrane potential to examine whether mitochondrial membrane integrity is affected by AA. AA clearly recovered the number of mitochondria, which was observed as decreased membrane potential in METH-stimulated SH-SY5Y cells (Fig. 6d). A similar protective effect of AA on mitochondrial membrane integrity was also confirmed by flow cytometric analyses. When SH-SY5Y cells were treated with METH, green fluorescence increased from 1.8% in the normal control to 59.3%. The percentage of cells that fluoresced red decreased to 40.7% after METH treatment. In contrast, the red fluorescence increased to 72.6% after AA treatment compared with METH. Taken together, these results indicate that AA protects human dopaminergic cells against mitochondrial injury caused by METH.

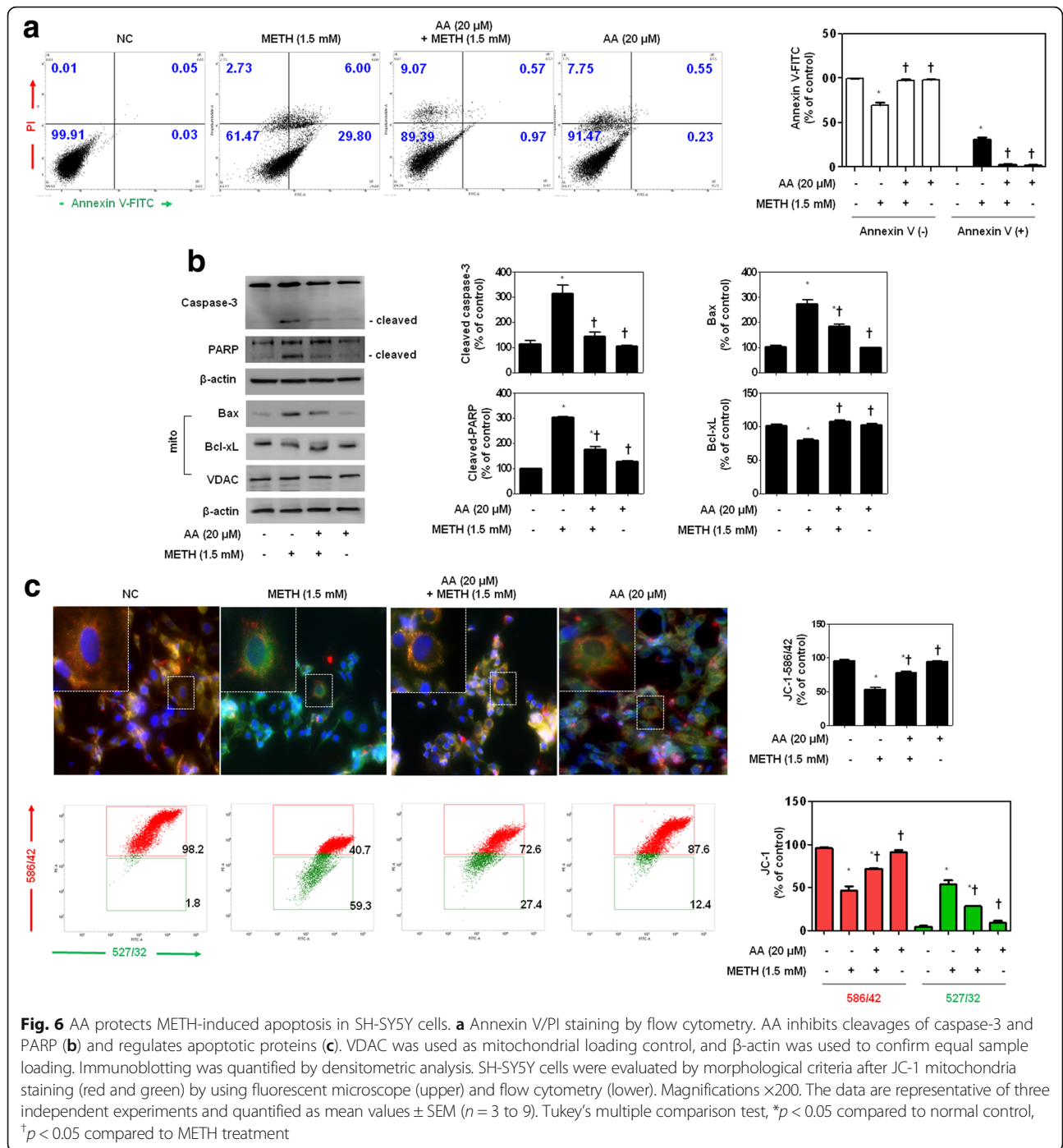




Discussion

Methamphetamine (METH) can act upon the neurons as a central processor of inflammation by releasing pro-

inflammatory molecules [7]. These pro-inflammatory molecules may further activate downstream apoptotic signaling pathways in neurons, ultimately resulting in



neuronal death and/or the activation of glial cells, which can further exacerbate neuroinflammation [2]. Therefore, inhibition of neurotoxicity and neuroinflammation by METH is important. Pro-inflammatory cytokines TNFα and IL-6 are key mediators of inflammatory responses associated with various neurological disorders including Parkinson's disease, Alzheimer's disease, and amyotrophic lateral sclerosis [14]. A high dose of METH

has been shown to induce TNFα and IL-6 in the striatum and hippocampus [1].

The major findings of this study are as follows: First, asiatic acid (AA) inhibits METH-induced TNFR overexpression and pro-inflammatory cytokine production in the dopaminergic SH-SY5Y cells. Second, METH-induced NF-κB and STAT3 translocation and ERK phosphorylation are prevented by AA pretreatment in

dopaminergic SH-SY5Y cells, mesencephalic neurons, and BV2 cells. Third, AA prevents METH-induced neurotoxicity through the mitochondria-dependent apoptotic pathway in dopaminergic SH-SY5Y cells.

TNF α is considered a potent stimulator of IL-6 production, whose pleiotropic action can be triggered through TNFR [9]. METH significantly increased the TNFR expression in dopaminergic SH-SY5Y cells. However, AA attenuated the elevation of METH-mediated TNFR expression in a concentration dependent.

METH has been found to be associated with neurotoxicity mediated by increased expression of pro-inflammatory cytokines such as TNF α and IL-6 [14]. These cytokines have also been suggested to play an important role in METH-induced brain dysfunction [1]. Our result showed that AA inhibits METH-induced secretion of TNF α and IL-6 and their mRNA expression in SH-SY5Y cells, mesencephalic neurons, and BV2 cells.

METH is able to induce pro-inflammatory cytokines and mediators through the NF- κ B and STAT3 pathways in dopaminergic and microglia cells [9, 15, 39]. The potential involvement of NF- κ B and STAT3 was investigated because the promoters of both TNF α and IL-6 contain binding sites for NF- κ B and STAT3, which are known to be involved in neurological disorders associated with increased inflammation [14, 18]. In accordance with these findings, our results showed that AA effectively inhibits nuclear translocation of NF- κ B (p65) and STAT3 in METH-stimulated dopaminergic SH-SY5Y cells, mesencephalic neurons, and BV2 cells. Thus, AA is likely to be a potent inhibitor of NF- κ B and STAT3 signaling.

Besides, MAPK signaling pathways play key roles in the induction of inflammatory cytokines by METH [40]. METH has been shown to affect phospho-ERK and p38 MAPK [41] and monocyte-derived dendritic cells [42]. ERK is a kinase that plays a role in regulating neuronal and behavioral processes mediated by dopamine and glutamate pathways [43]. Our results indicated that AA strongly inhibits METH-induced phosphorylation of ERK. However, AA did not participate in the inhibition of phosphorylation of p38.

Several lines of evidence suggest an important role of the intracellular signal transduction pathways in the mechanism of neural plasticity in response to drug abuse [44]. One of these signal transduction pathways is the ERK1/2 cascade, a member of the mitogen-activated protein kinase (MAPK) family. ERK1/2 activation can phosphorylate tyrosine hydroxylase (TH) and stimulate dopamine synthesis in the brain [45]. Accordingly, we found that phospho-ERK was most pronounced among all MAPKs after METH treatment. AA completely suppressed TH and phospho-ERK expression in TH-positive mesencephalic neurons. These results suggest

that AA regulated TH expression by the inhibition of ERK by METH.

METH-induced cell death contributes to the pathogenesis of neurotoxicity [46, 47]. Previous studies have suggested that apoptosis is a critical phenomenon involved in METH-induced neurotoxicity [11]. Putative mechanisms of METH-induced neurotoxicity have been proposed, including oxidative stress, excitotoxicity, and mitochondrial dysfunction followed by activation of caspase-3 with subsequent cleavage of PARP and DNA fragmentation, appearance of apoptotic cells, and dopaminergic degeneration [3, 48]. We evaluated the effect of AA on METH-induced neurotoxicity in dopaminergic SH-SY5Y cells to gain a better understanding of the molecular mechanisms involved in AA's anti-apoptotic effects. AA protected dopaminergic SH-SY5Y cells from apoptosis, as evaluated by assays of cell cycle arrest and mitochondrial membrane potential. Our results demonstrated that METH-induced cleavage of PARP was decreased through the inhibition of caspase-3 cleavage by AA. In addition, Bcl-xL was upregulated, whereas Bax was downregulated by AA in METH-induced neurotoxicity. The protective effects became more pronounced when the dopaminergic SH-SY5Y cells were treated with AA.

Conclusions

Our findings show that AA has a protective role against METH-induced neuroinflammation and neurotoxicity, specifically through inhibition of the NF- κ B/STAT3/ERK and mitochondria-mediated apoptosis pathway. Based on the literatures and our findings, AA is a promising candidate for anti-neurotoxic agent, and it can be used for the prevention and treatment of various neurological disorders.

Additional files

Additional file 1: Figure S1. Effects of AA and METH on the viability and morphology of SH-SY5Y cells. (a) SH-SY5Y cells were treated with AA (1, 5, 10, 15, 20, and 30 μ M) for 24 h, and then, MTT assays were conducted ($n = 4$). (b) SH-SY5Y cells were treated with METH (0.5, 1, 1.5, 2, and 5 mM) and then, MTT ($n = 4$) and ELISA assays ($n = 4$) were conducted. (c) SH-SY5Y cells were pretreated with AA (1, 10, and 20 μ M) for 1 h and then stimulated with 1 mM METH for 24 h. AA significantly increased the viability of 1 mM METH-stimulated SH-SY5Y cells in a concentration dependent ($n = 4$). (d) Cell morphology changes (magnifications $\times 200$, $n = 4$ /group). The data are representative of three independent experiments and quantified as mean values \pm SEM. Tukey's multiple comparison test, * $p < 0.05$ compared to normal control, $\dagger p < 0.05$ compared to METH treatment. (PDF 197 kb)

Additional file 2: Figure S2. Effects of AA on METH-induced translocation of NF- κ B and STAT3 in SH-SY5Y cells. Immunofluorescence double staining for p-NF- κ B p65 (green) and p-STAT3 (red) localization. Cells were counterstained with Hoechst 33342 (blue). Magnifications $\times 200$. The data are representative of three independent experiments. (PDF 83 kb)

Additional file 3: Figure S3. Effects of AA on METH-induced translocation of NF- κ B and TH expression in mesencephalic neurons. Immunofluorescence double staining for TH (green) and p-NF- κ B p65 (red) localization. Cells were counterstained with Hoechst 33342 (blue). Magnifications $\times 200$. The data are representative of three independent experiments. (PDF 154 kb)

Additional file 4: Figure S4. Effects of AA on METH-induced translocation of STAT3 and TH expression in mesencephalic neurons. Immunofluorescence double staining for TH (green) and p-STAT3 (red) localization. Cells were counterstained with Hoechst 33342 (blue). Magnifications $\times 200$. The data are representative of three independent experiments. (PDF 159 kb)

Additional file 5: Figure S5. METH induced neurotoxicity in dopaminergic SH-SY5Y cells. (a) The cell morphology by phase contrast to understand METH's neurotoxic effect. (b) Cleaved caspase-3 and PARP were increased with METH treatment. β -actin was used to confirm equal sample loading. The data are representative of three independent experiments and quantified as mean values \pm SEM. Tukey's multiple comparison test, * $p < 0.05$ compared to normal control. (PDF 174 kb)

Abbreviations

AA: Asiatic acid; ERK: Extracellular signal-regulated kinase; IL: Interleukin; MAPK: Mitogen-activated protein kinase; METH: Methamphetamine; NF- κ B: Nuclear factor kappa-light-chain-enhancer of activated B cells; PD: Parkinson's disease; STAT: Signal transducer and activator of transcription; TH: Tyrosine hydroxylase; TNF: Tumor necrosis factor; TNFR: Tumor necrosis factor receptor

Acknowledgements

Asiatic acid was purified and received from Dr. Ki Yong Lee, a professor of the College of Pharmacy, Korea University. BV-2 microglia cells and mesencephalic neuron cultures protocols was provided from Dr. Hoe Hyang-Sook, Korea Brain Research Institute, KBRI.

Funding

This research was supported by Basic Science Research Program through the National Research Foundation of Korea (NRF) funded by the Ministry of Education (NRF-2016R1A6A1A03011325).

Availability of data and materials

The datasets generated during and/or analyzed during the current study will be available upon request from the corresponding author.

Authors' contributions

JHP and BP designed and performed the experiments. YHS and JHJ provided the reagents. CHJ and SL analyzed the results. All authors read and approved the final manuscript.

Ethics approval

Experimental procedures were approved by the Institutional Animal Care and Use Committee of the Keimyung University in accordance with the criteria outlined in the Institutional Guidelines for Animal Research.

Consent for publication

Not applicable.

Competing interests

The authors declare that they have no competing interests.

Publisher's Note

Springer Nature remains neutral with regard to jurisdictional claims in published maps and institutional affiliations.

Author details

¹College of Pharmacy, Keimyung University, 1095 Dalgubeoldaero, Dalseo-Gu, Daegu 42601, Republic of Korea. ²Department of Pharmacology, School of Medicine, Keimyung University, 1095 Dalgubeoldaero, Dalseo-Gu, Daegu 42601, Republic of Korea.

Received: 20 April 2017 Accepted: 22 November 2017

Published online: 11 December 2017

References

- Goncalves J, Baptista S, Martins T, Milhazes N, Borges F, Ribeiro CF, Malva JO, Silva AP. Methamphetamine-induced neuroinflammation and neuronal dysfunction in the mice hippocampus: preventive effect of indomethacin. *Eur J Neurosci*. 2010;31:315–26.
- Jumnonprakhon P, Govitrapong P, Tocharus C, Tungkum W, Tocharus J. Protective effect of melatonin on methamphetamine-induced apoptosis in glioma cell line. *Neurotox Res*. 2014;25:286–94.
- Shin EJ, Shin SW, Nguyen TT, Park DH, Wie MB, Jang CG, Nah SY, Yang BW, Ko SK, Nabeshima T, Kim HC. Ginsenoside Re rescues methamphetamine-induced oxidative damage, mitochondrial dysfunction, microglial activation, and dopaminergic degeneration by inhibiting the protein kinase Cdelta gene. *Mol Neurobiol*. 2014;49:1400–21.
- Morrow BA, Roth RH, Redmond DE, Elsworth JD. Impact of methamphetamine on dopamine neurons in primates is dependent on age: implications for development of Parkinson's disease. *Neuroscience*. 2011;189:277–85.
- Nguyen XK, Lee J, Shin EJ, Dang DK, Jeong JH, Nguyen TT, Nam Y, Cho HJ, Lee JC, Park DH, et al. Liposomal melatonin rescues methamphetamine-elicited mitochondrial burdens, pro-apoptosis, and dopaminergic degeneration through the inhibition PKCdelta gene. *J Pineal Res*. 2015;58:86–106.
- Wen D, An M, Gou H, Liu X, Liu L, Ma C, Cong B. Cholecystokinin-8 inhibits methamphetamine-induced neurotoxicity via an anti-oxidative stress pathway. *Neurotoxicology*. 2016;57:31–38.
- Dang DK, Shin EJ, Nam Y, Ryoo S, Jeong JH, Jang CG, Nabeshima T, Hong JS, Kim HC. Apocynin prevents mitochondrial burdens, microglial activation, and pro-apoptosis induced by a toxic dose of methamphetamine in the striatum of mice via inhibition of p47phox activation by ERK. *J Neuroinflammation*. 2016;13:12.
- Reiner DJ, Yu SJ, Shen H, He Y, Bae E, Wang Y. 9-Cis retinoic acid protects against methamphetamine-induced neurotoxicity in nigrostriatal dopamine neurons. *Neurotox Res*. 2014;25:248–61.
- Coelho-Santos V, Goncalves J, Fontes-Ribeiro C, Silva AP. Prevention of methamphetamine-induced microglial cell death by TNF-alpha and IL-6 through activation of the JAK-STAT pathway. *J Neuroinflammation*. 2012;9:103.
- Wang Q, Shin EJ, Nguyen XK, Li Q, Bach JH, Bing G, Kim WK, Kim HC, Hong JS. Endogenous dynorphin protects against neurotoxin-elicited nigrostriatal dopaminergic neuron damage and motor deficits in mice. *J Neuroinflammation*. 2012;9:124.
- Nam Y, Wie MB, Shin EJ, Nguyen TT, Nah SY, Ko SK, Jeong JH, Jang CG, Kim HC. Ginsenoside Re protects methamphetamine-induced mitochondrial burdens and proapoptosis via genetic inhibition of protein kinase C delta in human neuroblastoma dopaminergic SH-SY5Y cell lines. *J Appl Toxicol*. 2015;35:927–44.
- Ajjimaporn A, Shavali S, Ebadi M, Govitrapong P. Zinc rescues dopaminergic SK-N-SH cell lines from methamphetamine-induced toxicity. *Brain Res Bull*. 2008;77:361–6.
- Klongpanichapak S, Phansuwan-Pujito P, Ebadi M, Govitrapong P. Melatonin inhibits amphetamine-induced increase in alpha-synuclein and decrease in phosphorylated tyrosine hydroxylase in SK-N-SH cells. *Neurosci Lett*. 2008;436:309–13.
- Shah A, Silverstein PS, Singh DP, Kumar A. Involvement of metabotropic glutamate receptor 5, AKT/PI3K signaling and NF-kappaB pathway in methamphetamine-mediated increase in IL-6 and IL-8 expression in astrocytes. *J Neuroinflammation*. 2012;9:52.
- Permpoonputtana K, Govitrapong P. The anti-inflammatory effect of melatonin on methamphetamine-induced proinflammatory mediators in human neuroblastoma dopamine SH-SY5Y cell lines. *Neurotox Res*. 2013;23:189–99.
- Venkatesan R, Ji E, Kim SY. Phytochemicals that regulate neurodegenerative disease by targeting neurotrophins: a comprehensive review. *Biomed Res Int*. 2015;2015:814068.
- Scheller J, Chalaris A, Schmidt-Arras D, Rose-John S. The pro- and anti-inflammatory properties of the cytokine interleukin-6. *Biochim Biophys Acta*. 1813;2011:878–88.
- Wang K, Xie M, Zhu L, Zhu X, Zhang K, Zhou F. Ciliary neurotrophic factor protects SH-SY5Y neuroblastoma cells against Abeta1-42-induced neurotoxicity via activating the JAK2/STAT3 axis. *Folia Neuropathol*. 2015;53:226–35.

19. Cadet JL, Jayanthi S, Deng X. Methamphetamine-induced neuronal apoptosis involves the activation of multiple death pathways. Review. *Neurotox Res.* 2005;8:199–206.
20. Beauvais G, Atwell K, Jayanthi S, Ladenheim B, Cadet JL. Involvement of dopamine receptors in binge methamphetamine-induced activation of endoplasmic reticulum and mitochondrial stress pathways. *PLoS One.* 2011;6:e28946.
21. Wang SF, Yen JC, Yin PH, Chi CW, Lee HC. Involvement of oxidative stress-activated JNK signaling in the methamphetamine-induced cell death of human SH-SY5Y cells. *Toxicology.* 2008;246:234–41.
22. Xing B, Xin T, Zhao L, Hunter RL, Chen Y, Bing G. Glial cell line-derived neurotrophic factor protects midbrain dopaminergic neurons against lipopolysaccharide neurotoxicity. *J Neuroimmunol.* 2010;225:43–51.
23. Tsao SM, Yin MC. Antioxidative and antiinflammatory activities of asiatic acid, glycyrrhizic acid, and oleanolic acid in human bronchial epithelial cells. *J Agric Food Chem.* 2015;63:3196–204.
24. Craig SR, Takanishi DM Jr. Educational milestone development for transitional year residency training. *J Grad Med Educ.* 2014;6:355–7.
25. Nataraj J, Manivasagam T, Justin Thenmozhi A, Essa MM. Neuroprotective effect of asiatic acid on rotenone-induced mitochondrial dysfunction and oxidative stress-mediated apoptosis in differentiated SH-SY5Y cells. *Nutr Neurosci.* 2017;20:351–9.
26. Jiang W, Li M, He F, Bian Z, He Q, Wang X, Yao W, Zhu L. Neuroprotective effect of asiatic acid against spinal cord injury in rats. *Life Sci.* 2016;157:45–51.
27. Xu MF, Xiong YY, Liu JK, Qian JJ, Zhu L, Gao J. Asiatic acid, a pentacyclic triterpene in *Centella asiatica*, attenuates glutamate-induced cognitive deficits in mice and apoptosis in SH-SY5Y cells. *Acta Pharmacol Sin.* 2012;33:578–87.
28. Sirichoat A, Chajjaroonkhanarak W, Prachaney P, Pannangrong W, Leksomboon R, Chaichun A, Wigmore P, Welbat JU. Effects of asiatic acid on spatial working memory and cell proliferation in the adult rat hippocampus. *Nutrients.* 2015;7:8413–23.
29. Krishnamurthy RG, Senut MC, Zemke D, Min J, Frenkel MB, Greenberg EJ, Yu SW, Ahn N, Goudreau J, Kassab M, et al. Asiatic acid, a pentacyclic triterpene from *Centella asiatica*, is neuroprotective in a mouse model of focal cerebral ischemia. *J Neurosci Res.* 2009;87:2541–50.
30. Umka Welbat J, Sirichoat A, Chajjaroonkhanarak W, Prachaney P, Pannangrong W, Pakdeechote P, Sripanidkulchai B, Wigmore P. Asiatic acid prevents the deleterious effects of valproic acid on cognition and hippocampal cell proliferation and survival. *Nutrients.* 2016;8:303.
31. Pruszek J, Just L, Isacson O, Nikkha G. Isolation and culture of ventral mesencephalic precursor cells and dopaminergic neurons from rodent brains. *Curr Protoc Stem Cell Biol* 2009, Chapter 2:Unit 2D.5. doi:10.1002/9780470151808.sc02d05s11.
32. Park JH, Lee MK, Yoon J. Gamma-linolenic acid inhibits hepatic PAI-1 expression by inhibiting p38 MAPK-dependent activator protein and mitochondria-mediated apoptosis pathway. *Apoptosis.* 2015;20:336–47.
33. Park JH, Lee KY, Park B, Yoon J. Suppression of Th2 chemokines by crocin via blocking of ERK-MAPK/NF-kappaB/STAT1 signalling pathways in TNF-alpha/IFN-gamma-stimulated human epidermal keratinocytes. *Exp Dermatol.* 2015;24:634–6.
34. Carniglia L, Ramirez D, Durand D, Saba J, Turati J, Caruso C, Scimonelli TN, Lasaga M. Neuropeptides and microglial activation in inflammation, pain, and neurodegenerative diseases. *Mediat Inflamm.* 2017;2017:5048616.
35. Sabio G, Davis RJ. TNF and MAP kinase signalling pathways. *Semin Immunol.* 2014;26:237–45.
36. McArthur S, Cristante E, Paterno M, Christian H, Roncaroli F, Gillies GE, Solito E. Annexin A1: a central player in the anti-inflammatory and neuroprotective role of microglia. *J Immunol.* 2010;185:6317–28.
37. Skaper SD, Mercanti G, Facci L. Culture and characterization of rat mesencephalic dopaminergic neurons. *Methods Mol Biol.* 2012;846:91–101.
38. Shin EJ, Dang DK, Tran TV, Tran HQ, Jeong JH, Nah SY, Jang CG, Yamada K, Nabeshima T, Kim HC. Current understanding of methamphetamine-associated dopaminergic neurodegeneration and psychotoxic behaviors. *Arch Pharm Res.* 2017;40:403–28.
39. Robson MJ, Turner RC, Naser ZJ, McCurdy CR, O'Callaghan JP, Huber JD, Matsumoto RR. SN79, a sigma receptor antagonist, attenuates methamphetamine-induced astrogliosis through a blockade of OSMR/gp130 signaling and STAT3 phosphorylation. *Exp Neurol.* 2014;254:180–9.
40. Wang X, Wang C, Wang J, Zhao S, Zhang K, Wang J, Zhang W, Wu C, Yang J. Pseudoginsenoside-F11 (PF11) exerts anti-neuroinflammatory effects on LPS-activated microglial cells by inhibiting TLR4-mediated TAK1/IKK/NF-kappaB, MAPKs and Akt signaling pathways. *Neuropharmacology.* 2014;79:642–56.
41. Yan T, Li L, Sun B, Liu F, Yang P, Chen T, Li T, Liu X. Luteolin inhibits behavioral sensitization by blocking methamphetamine-induced MAPK pathway activation in the caudate putamen in mice. *PLoS One.* 2014;9:e98981.
42. Nair MP, Saiyed ZM, Nair N, Gandhi NH, Rodriguez JW, Boukli N, Provencio-Vasquez E, Malow RM, Miguez-Burbano MJ. Methamphetamine enhances HIV-1 infectivity in monocyte derived dendritic cells. *J Neuroimmune Pharmacol.* 2009;4:129–39.
43. Shiflett MW, Balleine BW. Contributions of ERK signaling in the striatum to instrumental learning and performance. *Behav Brain Res.* 2011;218:240–7.
44. Nestler EJ. Molecular basis of long-term plasticity underlying addiction. *Nat Rev Neurosci.* 2001;2:119–28.
45. Mizoguchi H, Yamada K, Mizuno M, Mizuno T, Nitta A, Noda Y, Nabeshima T. Regulations of methamphetamine reward by extracellular signal-regulated kinase 1/2/ets-like gene-1 signaling pathway via the activation of dopamine receptors. *Mol Pharmacol.* 2004;65:1293–301.
46. Matsumoto RR, Nguyen L, Kaushal N, Robson MJ. Sigma (sigma) receptors as potential therapeutic targets to mitigate psychostimulant effects. *Adv Pharmacol.* 2014;69:323–86.
47. Huang YN, Yang LY, Wang JY, Lai CC, Chiu CT, Wang JY. L-Ascorbate protects against methamphetamine-induced neurotoxicity of cortical cells via inhibiting oxidative stress, autophagy, and apoptosis. *Mol Neurobiol.* 2017;54:125–36.
48. Shin EJ, Duong CX, Nguyen XK, Li Z, Bing G, Bach JH, Park DH, Nakayama K, Ali SF, Kanthasamy AG, et al. Role of oxidative stress in methamphetamine-induced dopaminergic toxicity mediated by protein kinase Cdelta. *Behav Brain Res.* 2012;232:98–113.

Submit your next manuscript to BioMed Central and we will help you at every step:

- We accept pre-submission inquiries
- Our selector tool helps you to find the most relevant journal
- We provide round the clock customer support
- Convenient online submission
- Thorough peer review
- Inclusion in PubMed and all major indexing services
- Maximum visibility for your research

Submit your manuscript at
www.biomedcentral.com/submit

